

Geochemistry of carbonatites in Maoniuping REE deposit, Sichuan Province, China

XU Cheng (许成)^{1,2}, HUANG Zhilong (黄智龙)¹, LIU Congqiang (刘丛强)¹,
QI Liang (漆亮)¹, LI Wenbo (李文博)¹ & GUAN Tao (管涛)¹

1. Open Laboratory of Ore Deposit Geochemistry, Institute of Geochemistry, Chinese Academy of Sciences, Guiyang 550002, China;

2. Graduate School, Chinese Academy of Sciences, Beijing 100039, China

Correspondence should be addressed to Xu Cheng (email: xucheng1999@hotmail.com)

Received April 14, 2002

Abstract Carbonatites in the Maoniuping REE deposit, Sichuan Province, which are spatially and temporally associated with rare earth mineralization, were emplaced at the time of Himalayan. The rocks are carbonatite-syenite complexes, with the mineral assemblages of calcite-aegirine-acmite-arfvedsonite-mica-orthoclase. The rocks are characterized by the enrichment in incompatible elements, such as Sr, Ba and REE, with C and O isotopic compositions of the "primary igneous carbonatites", relatively high initial $^{87}\text{Sr}/^{86}\text{Sr}$ ratios and low ϵ_{Nd} values. All of these suggest that the rocks were derived from the metasomatic enriched mantle. It is demonstrated by geological and geochemical evidence that the mixing of the Himalayan subducting crustal materials with mantle source EM1 is probably the main factor responsible for the formation of carbonatites. The carbonatite-syenite complexes were generated from liquid immiscibility of CO_2 -rich alkalic silicate magma, which was derived from partial melting of the metasomatic mantle.

Keywords: carbonatite, geochemistry, EM1-EM2, Maoniuping REE deposit.

Carbonatites are rarely igneous rocks distributed on the earth. The rocks usually form ring complexes with alkalic rocks, occurring in the environments of continental rift, collisional orogenic zone and oceanic island^[1, 2]. Numerous facts and experiments have revealed^[3-5] that the parental magma of carbonatites originated from the metasomatic enriched mantle; compared with silicate melts, carbonatite melts are characterized by the relative enrichment in volatile components, low solidus and liquidus temperatures, viscosities, densities, and high mobility of carbonatite magma relatively little contaminated by crustal materials during magma emplacement or eruption. The rocks are closely associated with REE, Nb, P, Fe and Th. Thus, comprehensive investigations of carbonatites are very important for a better understanding of mantle metasomatism, the origin and evolution of magma and related mineralization.

Although carbonatites have been found in many parts of China, such as Miaoya of Hubei Province, Zijinshan of Shanxi Province, Dashigou of Shaanxi Province, Fanshan of Hebei Province, central Shandong Province, Bayan Obo of Inner Mongolia and Maoniuping of Sichuan Province^[6], relatively little work has been published on the geochemistry and petrogenesis of the rocks. Carbonatites are closely associated with rare earth mineralization in Maoniuping, Sichuan

Province. Some petrological and geochemical features of the rocks were reported by Pu^[7] and Wang et al^[8]. In this paper, we systematically analyze the compositions of major elements, trace elements and isotopes, and discuss the characteristics of carbonatite source and genetic relationship between carbonatites and syenites.

1 Geological settings and fundamental features of carbonatites

The Maoniuping REE deposit is located in the northern Panxi rift. The area is divided into the east rift zone, the middle transitional zone and the west geosyncline fold zone by the NE-trending Nanhe fault and the Jingpingshan fault, and the Maoniuping REE deposit is located in the middle transitional zone. In the area are primarily distributed the Middle Devonian silt-clasolite, carbonate and the Quaternary proluvium and talus. The main structure is the NE-trending fault. Magmatites are distributed extensively in this area, including Yanshanian granites (Mianxi granites), Himalayan syenites and minor basalts and rhyolites of unknown ages^[9].

Vein-like carbonatites intruded into the center of syenites, with the attitude generally in consistence with the NE-trending fault. Veinlets on both sides of the main vein also intruded into syenites (fig. 1). The carbonatite veins (90—200 m wide) extend 400 m without pinching. Carbonatites are mostly composed of calcite (>90%), with minor amounts of biotite, aegirine, acmite, arfvedsonite, orthoclase, etc. (<10%), and the accessory minerals such as apatite, arpidelite etc. (<1%). On the margins of carbonatite veins the fenitization and arfvedsonitization are developed. According to Pu^[10], the K-Ar age of carbonatites is about (31.7±0.7) Ma, which is generally equivalent to that of syenites ((27.8±0.5)—(40.3±0.7) Ma).

2 Samples and analytical methods

Fresh calcites were selected from carbonatites and analyzed for major elements, trace elements and isotopes. The major elements of syenites and calcites were determined by using the wet-chemical method at the Institute of Geochemistry, the Chinese Academy of Sciences. The trace elements were analyzed by ICP-MS with the precision being better than 10%, also at the Institute of Geochemistry, the Chinese Academy of Sciences. The published paper^[11] can be referred to for the details of the analytical procedure. In the processes of analysis the international standard AMH-1 (andesite) was used as the standard specimen for quality control. The C and O isotopic compositions were analyzed at the Institute of Geology, the Chinese Academy of Geological Sciences (CAGS) by the 100% phosphorate method on the MAT 251 EM mass spectrometer, with the analytical precision being ±0.2‰. The Sr and Nd isotopic compositions were analyzed at the Institute of Geology and Geophysics, the Chinese Academy of Sciences. The analytical procedures for Sr and Nd isotopes were similar to each other. Samples were first dissolved in HF+HClO₄, then Rb, Sr and REE were separated on the AGW50×12 (100—200 meshes) cation exchange columns and were dried, respectively. The REE were further dissolved in 200 μL of 0.1 mol/L HCl solution, then Sm and Nd were separated on the levextrel resin ion exchange columns.

The blanks were $Rb=50 \times 10^{-11}$ g/g, $Sr=50 \times 10^{-11}$ g/g, $Sm=7 \times 10^{-11}$ g/g and $Nd=8 \times 10^{-11}$ g/g. NBS987 and LA standards analyzed during this work gave $^{87}Sr/^{86}Sr=0.710234 \pm 7$ and $^{143}Nd/^{144}Nd=0.511838 \pm 8$.

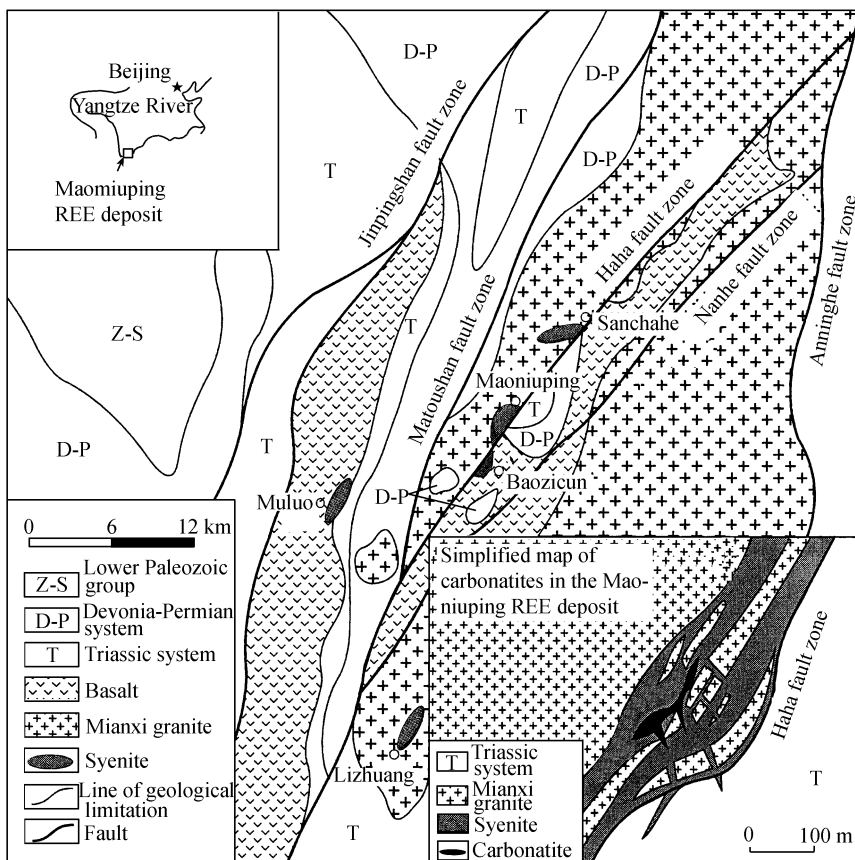


Fig. 1. Simplified geological map of the Maoniuping REE deposit. The map is revised according to data from No. 109 Geological Party.

3 Geochemistry

3.1 Major elements

Listed in table 1 are the major element contents of carbonatites in the Maoniuping mineral district. The concentrations of SiO_2 range from 1.67% (weight percent) to 3.65% (weight percent, the same hereafter), and the contents of CaO, MgO and Fe_2O_3+FeO range from 54.20% to 55.50%, 0.01% to 0.20%, and 0.20% to 0.36%, respectively. The contents of Na_2O and K_2O are extremely low (0.05%—0.08%, 0.001%—0.12%, respectively). The resulting data are fallen into the range of the major element contents of carbonatites reported by Samoiliv et al.^[12]. The $CaO/(CaO + MgO + FeO + Fe_2O_3 + MnO)$ ratios of 95.8%—98.5% are consistent with those of the calico-carbonatites.

Table 1 Contents of major elements (%), trace elements ($\times 10^{-6}$) of carbonatites and syenites

Sample No.	MNP -6	MNP -10	MNP -11	MNP -13	MNP -15	MNP -12-5	MNP -14-2	MNP -16-1	MNP -15-1	MNP -65	MNP -42	MNP -70	MNP -88
Type ^{a)}	Car	Car	Car	Car	Car	Car	Car	Car	Sye	Sye	Sye	Sye	Sye
SiO ₂	3.23	3.65	1.67	2.47	3.57	2.94	2.95	2.88	74.62	75.59	72.65	73.86	75.61
TiO ₂	0.001	0.002	0.001	0.002	0.001	0.001	0.002	0.001	0.42	0.02	0.15	0.37	0.03
Al ₂ O ₃	0.09	0.14	0.09	0.09	0.14	0.14	0.23	0.09	12.69	12.39	14.26	12.96	11.82
Fe ₂ O ₃	0.30	0.20	0.36	0.30	0.25	0.35	0.70	0.20	0.80	0.62	1.00	0.40	0.73
FeO	0.17	0.08	0.10	0.12	0.07	0.10	0.24	0.16	0.12	0.20	0.60	0.16	0.25
MnO	0.92	0.55	0.60	0.61	0.54	0.56	1.05	0.65	0.01	0.003	0.01	0.01	0.01
MgO	0.20	0.01	0.10	0.10	0.10	0.20	0.40	0.10	0.10	0.20	0.50	0.10	0.20
CaO	55.10	55.00	55.40	55.50	54.90	55.40	54.60	54.20	0.60	0.20	0.20	0.20	0.60
Na ₂ O	0.06	0.06	0.06	0.07	0.08	0.05	0.06	0.07	4.90	3.36	3.97	5.62	4.86
K ₂ O	0.001	0.02	0.01	0.02	0.01	0.01	0.09	0.12	3.13	4.80	3.96	3.74	3.34
P ₂ O ₅	0.001	0.002	0.001	0.001	0.002	0.002	0.001	0.001	0.001	0.001	0.001	0.002	0.001
H ₂ O ⁺	0.90	0.85	0.70	0.40	0.70	0.90	0.10	0.43	1.74	1.80	1.97	1.63	1.57
H ₂ O ⁻	0.05	0.07	0.05	0.05	0.05	0.05	0.03	0.05	0.10	0.15	0.15	0.10	0.15
CO ₂	38.10	38.50	40.10	39.90	39.50	38.62	39.00	40.20					
Total	99.12	99.13	99.24	99.63	99.91	99.32	99.45	99.18	99.25	99.33	99.42	99.15	99.17
Sr	10530	14150	10780	10840	14285	11788	15017	11676	268	30.8	58.2	403	244
Rb	0.18	0.50	0.26	0.30	0.45	0.18	0.50	1.15	167	221	174	136	159
Ba	1069	378	1629	1178	426	1371	497	1295	3109	287	987	1857	1810
Th	0.46	0.23	0.65	2.0	1.68	0.71	1.02	1.03	74.0	27.9	25.8	30.9	56.8
Ta	0.018	0.026	0.018	0.019	0.038	0.026	0.024	0.014	0.90	2.63	1.69	0.36	1.10
Nb	0.016	0.071	0.33	0.11	0.10	0.031	0.077	0.041	26.9	32.7	21.5	10.0	25.4
Zr	0.10	0.12	0.097	0.11	0.078	0.065	0.18	0.079	198	269	280	69.4	142
Hf	0.078	0.055	0.053	0.12	0.075	0.057	0.075	0.049	7.63	10.8	11.2	2.76	6.79
Y	156	131	148	150	152	138	156	133	15.8	53.0	31.4	16.4	17.7
Sc	2.30	2.03	2.45	2.23	2.19	1.92	1.77	1.91	0.72	2.13	2.72	0.70	0.47
La	454	648	523	827	785	475	794	513	198	95.4	385	215	136
Ce	916	1395	1143	1627	1707	1042	1730	1078	310	159	513	245	215
Pr	94.7	141	119	159	158	110	175	110	30.1	17.4	46.2	27.5	20.2
Nd	377	542	468	598	686	427	687	421	93.4	57.4	132	86.6	64.5
Sm	65.1	74.7	74.3	84.4	98.4	69.9	99.5	63.5	12.9	9.54	12.1	9.78	8.86
Eu	15.0	16.4	16.4	18.4	21.0	15.7	20.8	14.4	2.90	2.24	2.02	2.53	2.25
Gd	49.1	50.3	53.0	59.2	65.4	49.5	65.6	45.5	6.54	8.17	7.80	6.17	5.21
Tb	6.18	5.53	6.27	6.62	7.22	5.83	7.33	5.20	0.74	1.30	0.98	0.69	0.65
Dy	31.0	25.3	29.7	30.7	32.8	27.7	33.2	24.4	2.83	7.71	5.30	2.97	3.04
Ho	5.68	4.16	5.04	5.09	5.27	4.62	5.46	4.33	0.44	1.61	1.05	0.53	0.49
Er	17.3	12.7	15.1	15.8	16.1	13.9	16.2	13.1	1.06	4.89	3.08	1.23	1.22
Tm	2.38	1.53	1.94	1.97	1.96	1.78	1.99	1.65	0.14	0.75	0.48	0.15	0.17
Yb	15.7	10.1	12.0	12.6	12.6	11.4	12.7	10.8	0.94	5.80	3.58	1.02	1.22
Lu	2.03	1.24	1.53	1.57	1.45	1.40	1.55	1.33	0.11	0.87	0.53	0.13	0.17

a) Car stands for carbonatite, and Sye for syenite.

3.2 Trace elements

In comparison with the average values of the world calcio-carbonatites^[13], those of the rocks in the Maoniuping area are characterized by relatively low Nb and Ta contents and relatively high Sr/Sm, Zr/Hf, Sm/Hf, Nb/Ta and La/Nb ratios (128—183, 1.04—2.44, 703—1401, 1.20—18.4 and 7526—28380, respectively). It is shown in fig. 2 that carbonatites in the Maoniuping area relatively enrich Ba, Sr and LREE, and deplete Nb, Ta, Zr, Hf and Ti.

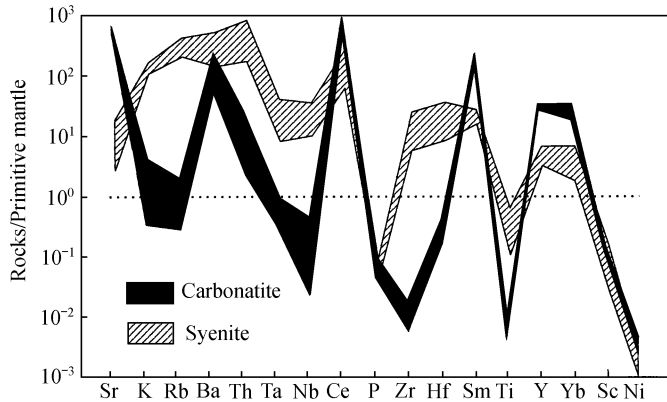


Fig. 2. Primitive mantle-normalized trace elements of carbonatites and syenites in the Maoniuping orefield. The values of primitive mantle are cited from ref. [14].

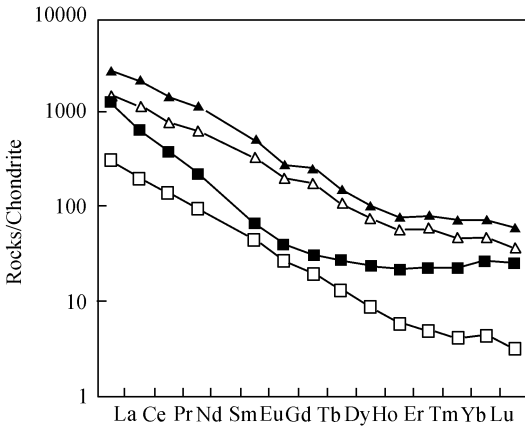


Fig. 3. Chondrite-normalized REE distribution patterns of carbonatites and syenites in the Maoniuping orefield. The data of chondrites are cited from ref. [15]. The solid area stands for the highest contents of REE, and the hollow area indicates the lowest contents of REE. Δ , \blacktriangle , calcites; \square , \blacksquare , syenites.

The Σ REE contents of carbonatites range from 2051×10^{-6} to 3652×10^{-6} , with LREE and HREE concentrations ranging from 1922×10^{-6} to 3508×10^{-6} and 106×10^{-6} to 144×10^{-6} , respectively. The LREE/HREE ratios range from 14 to 25. The chondrite-normalized REE distribution patterns are of the LREE enrichment type (fig. 3), with $(\text{La}/\text{Yb})_n = 23.1\text{—}44.4$, $(\text{La}/\text{Nd})_n = 2.09\text{—}2.68$, $(\text{Gd}/\text{Yb})_n = 2.53\text{—}4.18$, and show weak negative Eu anomalies ($\delta\text{Eu} = 0.79\text{—}0.82$), and unremarkable Ce anomalies ($\delta\text{Ce} = 0.88\text{—}1.06$). It is also shown in fig. 3 that the chondrite-normalized REE distribution patterns of carbonatites are similar to those of syenites with $(\text{La}/\text{Yb})_n = 72\text{—}213$, $(\text{La}/\text{Nd})_n = 3.80\text{—}4.80$, $(\text{Gd}/\text{Yb})_n = 3.45\text{—}7.93$, $\delta\text{Eu} = 0.86\text{—}1.01$, and $\delta\text{Ce} = 0.77\text{—}1.02$, except that the former rocks enrich HREE, with low $(\text{Gd}/\text{Yb})_n$ ratios.

3.3 C and O isotopes

The C and O isotopic compositions of carbonatites in the Maoniuping REE deposit are relatively constant (table 2), with the $\delta^{13}\text{C}_{\text{PDB}}$ and $\delta^{18}\text{O}_{\text{SMOW}}$ values in the range of -6.6‰ — -7.0‰ , and 6.4‰ — 7.4‰ , respectively. The maximum differences are 0.4‰ and 1.0‰ , respectively. They are fallen into the range of the “primary igneous carbonatites” (the $\delta^{13}\text{C}_{\text{PDB}}$ and $\delta^{18}\text{O}_{\text{SMOW}}$ values being -4‰ — -8‰ , 6‰ — 10‰ , respectively)^[16].

3.4 Sr and Nd isotopes

The Sr and Nd isotopic compositions of carbonatites are similar to those of syenites, and the values of initial $^{87}\text{Sr}/^{86}\text{Sr}$, $^{143}\text{Nd}/^{144}\text{Nd}$, ϵ_{Sr} and ϵ_{Nd} of carbonatites are in the range of 0.706074 — 0.706149 , 0.512383 — 0.512406 , 22.9 — 23.9 , and -4.2 — -3.7 , respectively (table 3), against 0.705972 — 0.706302 , 0.512378 — 0.512405 , 21.4 — 26.1 , and -4.2 — -3.7 , respectively, for the latter rocks. In the ϵ_{Nd} vs. initial $^{87}\text{Sr}/^{86}\text{Sr}$ diagram, the values lie in the narrow range between EM1 and EM2, relatively close to EM1. It is also indicated that carbonatites and syenites of the Maoniuping orefield are fallen into the same area.

Table 2 C and O isotopic contents of carbonatites^{a)}

Sample No.	$\delta^{13}\text{C}_{\text{PDB}} (\text{‰})$	$\delta^{18}\text{O}_{\text{PDB}} (\text{‰})$	$\delta^{18}\text{O}_{\text{SMOW}} (\text{‰})$
MNP-15	-7.0	-23.4	6.7
MNP-6	-6.8	-22.9	7.2
MNP-11	-6.6	-23.8	6.4
MNP-10	-6.6	-22.8	7.4
MNP-13	-6.7	-23.0	7.2
MNP-142	-6.9	-23.1	7.1
MNP-16-1	-6.7	-22.9	7.2
MNP-125	-6.8	-23.2	6.9

a) Samples were analyzed at the Institute of Geology, CAGS. The formula for calculating $\delta^{18}\text{O}_{\text{SMOW}}$ values is from Friedman^[17]: $\delta^{18}\text{O}_{\text{SMOW}} = 1.03086 \times \delta^{18}\text{O}_{\text{PDB}} + 30.86$.

Table 3 Sr and Nd isotopic contents of carbonatites and syenites^{a)}

Sample No.	MNP-10	MNP-135	MNP-16-1	MNP-125
Rock type	carbonatite	carbonatite	carbonatite	carbonatite
$^{87}\text{Rb}/^{86}\text{Sr}$	2.14E-05	7.32E-05	5.40E-05	5.19E-05
$^{87}\text{Sr}/^{86}\text{Sr}$	0.706075 ± 10	0.706074 ± 14	0.706075 ± 12	0.706149 ± 16
$(^{87}\text{Sr}/^{86}\text{Sr})_0$	0.706075	0.706074	0.706075	0.706149
ϵ_{Sr}	22.9	22.9	22.9	23.9
$^{147}\text{Sm}/^{144}\text{Nd}$	0.08884	0.09456	0.1001	0.09825
$^{143}\text{Nd}/^{144}\text{Nd}$	0.512414 ± 9	0.512411 ± 6	0.512405 ± 6	0.512411 ± 5
$(^{143}\text{Nd}/^{144}\text{Nd})_0$	0.512394	0.512390	0.512383	0.512389
ϵ_{Nd}	-3.9	-4.0	-4.2	-4.0
Sample No.	MNP-142	MNP-15-1	MNP-24	MNP-88
Rock type	carbonatite	syenite	syenite	syenite
$^{87}\text{Rb}/^{86}\text{Sr}$	9.54E-05	1.77	0.8965	1.541
$^{87}\text{Sr}/^{86}\text{Sr}$	0.706113 ± 10	0.706796 ± 12	0.706719 ± 11	0.706863 ± 14
$(^{87}\text{Sr}/^{86}\text{Sr})_0$	0.706113	0.705972	0.706302	0.706146
ϵ_{Sr}	23.4	21.4	26.1	23.9
$^{147}\text{Sm}/^{144}\text{Nd}$	0.09426	0.07796	0.05883	0.05675
$^{143}\text{Nd}/^{144}\text{Nd}$	0.512427 ± 7	0.512422 ± 9	0.512391 ± 10	0.512391 ± 9
$(^{143}\text{Nd}/^{144}\text{Nd})_0$	0.512406	0.512405	0.512378	0.512378
ϵ_{Nd}	-3.7	-3.7	-4.2	-4.2

a) Samples were analyzed at the Institute of Geology and Geophysics, CAS. Isotopic ratios are normalized to $\lambda_{\text{Rb}} = 1.41 \times 10^{-11} \text{ a}^{-1}$, $\lambda_{\text{Sm}} = 6.54 \times 10^{-12} \text{ a}^{-1}$, $(^{87}\text{Sr}/^{86}\text{Sr})_{\text{UR}} = 0.7045$, $(^{87}\text{Rb}/^{86}\text{Sr})_{\text{UR}} = 0.0816^{[18]}$, $(^{143}\text{Nd}/^{144}\text{Nd})_{\text{CHUR}} = 0.5123638$, $(^{147}\text{Sm}/^{144}\text{Nd})_{\text{CHUR}} = 0.1967^{[19]}$, as calculated by assuming an age of $30 \text{ Ma}^{[10]}$.

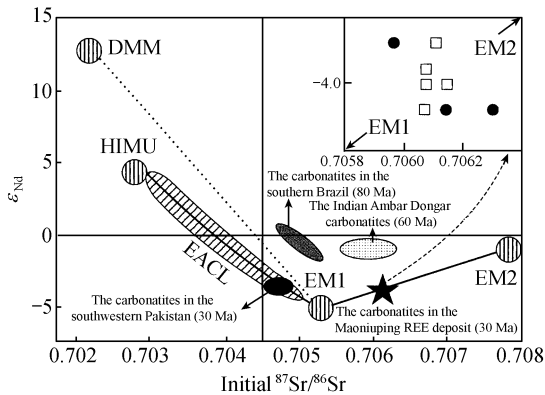


Fig. 4. ϵ_{Nd} vs. initial $^{87}Sr/^{86}Sr$ for carbonatites in the orefield. To limit the potential distortions caused by epsilon values, the comparison of Sr and Nd isotope is restricted to the foreign carbonatites younger than 100 Ma. The Brazilian data are cited from ref. [20], the Pakistani data from ref. [1], and the Indian data from ref. [21]. Squares stand for carbonatites, circles for syenites in the Maoniuping REE deposit. The range of EACL are cited from ref. [22]. DMM, HIMU, EM1, EM2 are the mantle end-member components from ref. [23], $(^{87}Sr/^{86}Sr)_{UR} = 0.7045$ [18].

from the Maoniuping area are fallen into the area between EM1 and EM2 in fig. 4, deviating from the EACL. They are characterized by high initial $^{87}Sr/^{86}Sr$ ratios, and low ϵ_{Nd} ratio values.

4 Discussion

4.1 Genesis of carbonatites and relationship between carbonatites and syenites

In the Maoniuping REE deposit, carbonatites are composed of calcite-aegirine-acmite-arfvedsonite-mica-orthoclase. The rocks are characterized by enrichment in incompatible elements, such as Sr, Ba, REE, with C and O isotopic compositions of the “primary igneous carbonatites”, Sr and Nd isotopic compositions fallen into the area between EM1 and EM2. All of these suggest that carbonatites are probably the products of mantle carbonate magma. Three genetic models for carbonatites are described as follows: (i) carbonatites are derived from low-degree partial melting (<1%) of CO_2 -rich asthenosphere or lithosphere mantle [22]; (ii) the rocks are the products of fractional crystallization of CO_2 -rich alkali silicate melt [24]; (iii) they are the products of liquid immiscibility of CO_2 -rich alkalic silicate melt [25, 26]. The evidence obtained from the present study supports the third viewpoint. Further discussions are given below:

(1) Consistent with the occurrences of other carbonatite-syenite complexes both at home and abroad [27], carbonatites in the Maoniuping area are closely associated in space with syenites, forming ring complexes with carbonatites at the center (fig. 1). Both rocks were emplaced approximately at the same time ((31.7 ± 0.7) Ma for carbonatites, (27.8 ± 0.5) to (40.3 ± 0.7) Ma for syenites) [10]. Besides, both rocks have similar chondrite-normalized REE distribution patterns (fig.

Viewing from the statistics data on the initial $^{87}Sr/^{86}Sr$ of carbonatites of different ages from the Six Continents, we found that initial Sr isotopic values tend to increase from the older carbonatites (2600 Ma) to younger ones (30 Ma), and their initial Sr isotopic compositions also tend to increase from 0.7015 to 0.7050. In contrast, the initial $^{87}Sr/^{86}Sr$ values of carbonatite from the Maoniuping REE deposit are higher, which apparently deviate from the above trend of variation. It is shown in fig. 4 that the young (<100 Ma) carbonatites in the world are mainly fallen into the area between HIMU and EM1 mantle end-member, consistent with the Sr and Nd isotopic compositions of the East African Carbonatites Line (EACL). The Sr and Nd isotopic compositions of carbonatites

3), and relatively constant Sr and Nd isotopic compositions (fig. 4). All these features suggest that they are probably derived from the same parental magma system.

(2) The two types of rocks have distinctive characteristics in both major elements and trace elements. As is shown in fig. 2, carbonatites are enrichment in Sr, La, etc., while syenites are relatively enriched in Rb, Zr, Hf, Nb and Ta. In their experiments, Veksler et al.^[28] reported that high field strength elements (Zr, Hf, Nb, Ta, Th, etc.) would partition preferentially into the silicate liquid, while large ion lithophile elements (Sr, La, etc.) would strongly partition into the carbonatite liquid during the liquid immiscibility of silicate-carbonatite melts. It is clear that the fractionation of trace elements between carbonatites and syenites in the Maoniuping area is consistent with the enrichment regularity of carbonatite-silicate complexes generated by liquid immiscibility.

(3) It was demonstrated by high temperature and high pressure experiments^[29] that REE would be relatively enriched in the carbonatite phase during carbonatite-silicate liquid immiscibility, and the values of $D_{\text{carbonatite/silicate}}$ (HREE) (partitioning coefficient) be larger than those of $D_{\text{carbonatite/silicate}}$ (LREE). Although the chondrite-normalized REE distribution patterns in carbonatites are similar to those of syenites, the former have higher total REE contents and more relative enrichment in HREE relative to the latter ((Gd/Yb)_n ratios of carbonatites and syenites being 2.53—4.18 and 3.45—7.93, respectively) (fig. 3). These features indicate that they are the products of liquid immiscibility of the same magmatic system.

(4) According to Harmer et al.^[22], in the carbonatite-alkalic rock complexes, if carbonatites were derived from low degree partial melting (less than 1%) of mantle, they would be characterized by relatively low ϵ_{Sr} and high ϵ_{Nd} values relative to the associated alkalic rocks if carbonatites were derived from liquid immiscibility of CO₂-rich silicate melt, then they would have similar ϵ_{Sr} and ϵ_{Nd} values to the associated silicate rocks. In the Maoniuping REE deposit, carbonatites and syenites have similar Sr and Nd isotopic compositions (table 3, fig. 4), implicating that they are the products of liquid immiscibility.

4.2 Characteristics of carbonatites source

Carbonatites in the Maoniuping REE deposit are characterized by enrichment in Ba, Sr and LREE, with high Sr/Sm, Zr/Hf, Nb/Ta and La/Nb ratios, relatively high initial $^{87}\text{Sr}/^{86}\text{Sr}$ and ϵ_{Sr} values, low initial $^{143}\text{Nd}/^{144}\text{Nd}$ and ϵ_{Nd} values, and they are fallen into the area narrowly close to EM1 in the ϵ_{Nd} -initial $^{87}\text{Sr}/^{86}\text{Sr}$ diagram. All of these demonstrate that the carbonatites were derived from the metasomatic enriched mantle^[30]. It was reported^[1] that among the young (<100 Ma) carbonatites worldwide, high initial Sr isotopic ratios (≥ 7.06) were only found in some carbonatites in Indian Ambar Dangar, and negative values of ϵ_{Nd} in the southern Brazil (80 Ma), Indian Ambar Dangar, southwestern Pakistan and the African rift (0 to 100 Ma). Carbonatites in the southwestern Pakistan and the African rift are fallen within the range of EACL (fig. 4). Negative ϵ_{Nd} values are attributed to the mixing of mantle end-member between HIMU and EM1, while carbonatites in the Indian Ambar Dangar and southern Brazil deviate from the range of EACL (fig.

4). Toyoda et al.^[20] and Simonetti et al.^[21] proposed that negative ϵ_{Nd} values could be explained by the contamination of the mantle source (DMM or HIMU) with lower crustal compositions. Carbonatites in the Maoniuping area ((31.7±0.7) Ma) are obviously different from the above-mentioned carbonatites with ages less than 100 Ma, fallen into the area between EM1 and EM2, relatively close to the EM1, deviating from the EACL range in ϵ_{Nd} vs. initial $^{87}\text{Sr}/^{86}\text{Sr}$ diagram (fig. 4).

Because the origin of EM2 compositions is related with subducting and recycling continental materials^[31], there are two explanations for Sr and Nd isotopic compositions of carbonatites in the studied area: First, the primitive magma derived from EM1 is contaminated by crustal materials during its ascending. Second, the EM1 mantle source is mixed with the subducting crustal materials. The major elements and REE contents of carbonatites in the Maoniuping area are relatively constant. Initial $^{87}\text{Sr}/^{86}\text{Sr}$, $^{143}\text{Nd}/^{144}\text{Nd}$, $\delta^{13}\text{C}_{\text{PDB}}$ and $\delta^{18}\text{O}_{\text{SMOW}}$ values of the rocks show little variation. These features suggest that the primitive magma is little contaminated by crustal materials in the process of ascending. For this reason, the first explanation can be ruled out. That is to say, the mantle source of the Maoniuping carbonatites was mixed with subducting crustal materials. So carbonatites were formed in a subduction environment instead of a rift environment. Although the deduction requires more geological and geochemical investigations, the following facts support the conclusion.

(1) Although the Maoniuping carbonatites occur in the Panxi rift, they were emplaced during the Himalayan period when the Panxi rift closed^[32]. Affected by the collision between the Indian plate and the Yangtze plate, a strongly orogenic movement is expected in this area during the Himalayan period, and inevitably the intracontinental subduction would take place, as supported by the evidence provided by Wang et al.^[8].

(2) It has been documented^[33–36] that the depth of intracontinental subduction could exceed the Moho, even reach the mantle, thereby inducing partial melting of the mantle materials. The studied area is located in the transitional zone between the Panxi rift and the Longmenshan-Jinpingshan orogenic zone, where the Yangtze plate penetrated as a wedge into the crust at Longmenshan, resulting in the Moho dislocation. The subduction event took place during the Himalayan period^[37, 38]. Using the “upper thrusting and lower wedging” model, Luo^[38] explained successfully the evolution of tectonics-magma-ore-deposition system in the Himalayan Longmenshan-Jinpingshan orogenic zone. According to this model, the intracontinental subduction event should have taken place in the Maoniuping area during the Himalayan period.

(3) The “TNT”-shaped anomalies in the incompatible elements distribution patterns of carbonatites and syenites in the Maoniuping REE deposit (fig. 2) also support the Himalayan subduction event^[39].

Acknowledgements Geological field work was greatly supported by Senior Engineer Pu Guangping of No. 109 Geology Party of the Department of Geology of Sichuan Province. Prof. Wand Denghong and Prof. Yuan Zhongxin offered valuable data. Here the authors wish to thank them all. This work was supported by the State Climbing Program (Grant No. 95-Pre-39).

References

1. Tilton, G. R., Bryce, J. G., Mategan, A., Pb-Sr-Nd isotope data from 30 and 300 Ma collision zone carbonatites in Northwest Pakistan, *J. Petrol.*, 1998, 39: 1865—1874.
2. Le Bas, M. J., Diversification of carbonatites, in *Carbonatites: Genesis and Evolution* (ed. Bell, K.), London: Unwin Hyman, 1989, 427—447.
3. Dobson, D. P., Jones, A. P., *In-situ* measurement of viscosity and density of carbonate melts at high pressure, *Earth Planet. Sci. Lett.*, 1996, 143: 207—215.
4. Wyllie, P. J., Origin of carbonatites: evidence from phase equilibrium studies, in *Carbonatites: Genesis and Evolution* (ed. Bell, K.), London: Unwin Hyman, 1989, 15—37.
5. Treiman, A. H., Schedl, A., Properties of carbonatite magma and processes in carbonatite magma chambers, *J. Petrol.*, 1983, 91: 437—447.
6. Tu Guangchi, The unique nature in ore composition, geological background and metallogenic mechanism of non-conventional super-large ore deposits: A preliminary discussion, *Science in China, Ser. D*, 1998, 41(Supplement), 1—6.
7. Pu, G. P., Discovery of an alkali pegmatite-carbonatite complex zone in Maoniuping, Southwestern Sichuan Province, *Geological Review* (in Chinese), 1988, 34(1): 86—92.
8. Wang, D. H., Yang, J. M., Yan, S. H., A special orogenic type REE deposit in Maoniuping, Sichuan, China: *Geology and geochemistry, Resource Geology*, 2001, 51(3): 177—188.
9. Yuan, Z. X., Shi, Z. M., Bai, G. et al., Rare Earth Element Deposit in Maoniuping Mianning in Sichuan Province (in Chinese), Beijing: Geological Publishing House, 1995, 89—102.
10. Pu, G. P., The evolution history of REE mineralization and major features of Himalayan REE deposit in the Panzhihua-Xichang area, Sichuan, in *Study on Himalayan endogenic mineralization* (eds. Chen, Y. C. , Wang, D. H.) (in Chinese), Beijing: Geological Publishing House, 2001, 104—116.
11. Qi, L., Hu, J., Gregoire, D. C., Determination of trace elements in granites by inductively coupled plasma mass spectrometry, *Talanta*, 2000, 51: 507—513.
12. Samoilov, V. S., The main geochemical features of carbonatites, *Journal of Geochemical Exploration*, 1991, 40: 251—262.
13. Yang, X. M., Yang, X. Y., Geological and geochemical characteristics of carbonatites and their implication for tectonic settings, *Advance in Earth Sciences* (in Chinese), 1998, 13(5): 457—466.
14. Sun, S. S., McDonough, W. F., Chemical and isotopic systematics of oceanic basalts: Implications for mantle compositions and processes, in *Migmatism in the Oceanic Basins*, Geological Society (ed. Saunders, A. D.), London: Special Publication, 1989, 313—345.
15. Boynton, W. V. , Cosmochemistry of the rare earth elements: Meteorite studies, *Dev. Geochem.*, 1984, 2: 63—114.
16. Keller, J., Hoefs, J., Stable isotope characteristics of recent natrocarbonatites from Oldoinyo Lengai, in *Carbonatites Volcanism: Oldoinyo Lengai and Petrogenesis of Natrocarbonatites*, IAVCEI Proceeding in Volcanology (ed. Bell, K.), Berlin: Springer, 1995, 113—123.
17. Friedman, I., Oneil, J. R., Compilation of stable isotope fractionation fraction factors of geochemical interest, in *Data of Geochemistry* (ed. Fleischer, M.), 6th ed., Geology Survey Professional Paper, 1977, 117—117.
18. Paolo, D. J., Implications of correlated Nd and Sr isotopic variations for the chemical evolution of crust and mantle, *Earth Planet. Sci. Lett.*, 1979, 43: 201—211.
19. Jachson, S. B., Wasserburg, J. G., Sm-Nd isotopic evolution of chondrites, *Earth Planet. Sci. Lett.*, 1980, 50: 139—155.
20. Toyoda, K., Horuchi, H., Tokonami, M. , Dupal anomaly of Brazilian carbonatites: Geochemical correlations with hot-spots in the South Atlantic and implications for the mantle source, *Earth Planet. Sci. Lett.*, 1994, 126: 315—331.
21. Simonetti, A., Bell, K., Nd, Pd, and Sr isotope systematics of fluorite at the Amba Dongar carbonatite complex, India: Evidence for hydrothermal and crustal fluid mixing, *Econ. Geol.*, 1995, 90: 2018—2027.
22. Harmer, R. E., Gittins, J., The case for primary, mantle-derived carbonatite magma, *J. Petrol.*, 1998, 39: 1895—1903.
23. Hart, S. R., Hauri, E. H., Oschmann, L. A., Mantle plume and entrainment isotopic evidence, *Science*, 1992, 256: 517—520.
24. Lee, W. J., Wyllie, P. J., Experimental data bearing on liquid immiscibility, crystal fraction, and the origin of calcic-carbonatites and natrocarbonatites, *International Geology Review*, 1994, 36: 797—819.
25. Kjarsgaard, B. A., Hamilton, D. L., The genesis of carbonatites by immiscibility, in *Carbonatites: Genesis and Evolution*

- (ed. Bell, K.), London: Unwin Hyman, 1989, 388—404.
26. Huang, Z. L., Liu, C. Q., Xiao, H. Y. et al., Study on the carbonate ocelli-bearing lamprophyre dyke in the Ailaoshan gold deposit zone, Yunnan Province, *Science in China, Ser. D*, 2002, 45(6): 494—502.
 27. Bell, K., Radiogenic isotope constraints on relationships between carbonatites and associated silicate rocks—A brief review, *J. Petrol.*, 1998, 39: 1987—1996.
 28. Veksler, I. V., Petibon, C., Jenner, G. A., Trace element partitioning in immiscible silicate-carbonate liquids: An initial experimental study using a centrifuge autoclave, *J. Petrol.*, 1998, 39: 2095—2104.
 29. Wendlandt, R. F., Harrison, W. J., Rare earth partitioning between immiscible carbonate and silicate liquids and CO₂ vapor: results and implications for the formation of light earth-enriched rocks, *Contrib. Mineral. Petrol.*, 1979, 69: 409—419.
 30. Ionov, D. A., Dupuy, C., Oreilly, S. Y., Carbonated peridotite xenoliths from Spitsbergen: Implications for trace element signature of mantle carbonate metasomatism, *Earth Planet. Sci. Lett.*, 1993, 119: 283—297.
 31. Hart, S. R., Heterogeneous mantle domains: signatures, genesis and mixing chronologies, *Earth Planet. Sci. Lett.*, 1988, 90: 273—296.
 32. Zhang, Y. X., Lu, Y. N., Yang, C. X. et al., *The Panxi Rift* (in Chinese), Beijing: Geological Publishing House, 1988, 224—270.
 33. Hu, S. X., Zhao, Y. B., Lu, B. et al., Evidence for the Jiangsu-Shandong ultra-high-pressure metamorphic belt returning from the upper mantle to the earth surface in the Mesozoic-Cenozoic, *Acta Geologica Sinica* (in Chinese), 1997, 71(3): 245—253.
 34. Chen, Y. J., Constraints and their mechanism on the petrogenic and metallogenic model for collision orogenesis, *Earth Science Frontiers* (in Chinese), 1998, 5 (Supplement): 109—118.
 35. Sui, Y. H., Wang, H. H., Gao, X. L. et al., Ore fluid of the Tieluping silver deposit of Henan Province and its illustration of the tectonic model for collisional petrogenesis, metallogenesis and fluidization, *Science in China, Ser. D*, 2000, 43(Supplement): 108—121.
 36. Chen, Y. J., Li, C., Zhang, J., Sr and Nd isotopic characteristics of porphyries in the Qinling molybdenum deposit belt and their implication to genetic mechanism and type, *Science in China, Ser. D*, 2000, 43(Supplement): 82—94.
 37. Xu, Z. Q., Yang, J. S., Jiang, M. et al., Continental subduction and uplifting of the orogenic belts at the margin of the Qinghai-Tibet Plateau, *Earth Science Frontiers* (in Chinese), 1999, 6(3): 139—150.
 38. Luo, Y., Yu, R. L., Major features and dynamic model of the Himalayan tectonic-magmatism in the intracontinental orogenic belt in Longmenshan-Jinpingshan, Sichuan Province, in *Study on Himalayan Endogenic Mineralization* (in Chinese) (eds. Chen, Y. C., Wang, D. H.), Beijing: Geological Publishing House, 2001, 88—96.
 39. Rock, N. M. S., *Lamprophyres*, Glasgow: Blackie, 1990.